Effect of Angiotensin-Induced Hypertension on Rat Coronary Arteries and Myocardium

Filiberto Giacomelli, MD, Piero Anversa, MD, and Joseph Wiener, MD

Acute hypertension has been produced in rats by the intravenous infusion of angiotensin amide for 4 hours. Both control and hypertensive animals were injected intravenously prior to sacrifice with either horseradish peroxidase (HRP) or colloidal carbon. Epicardial arteries and blocks of ventricular myocardium containing intramyocardial arteries and arterioles have been processed for electron microscopy. HRP appears to penetrate the endothelium of epicardial arteries from control animals within vesicles that bypass endothelial junctions and empty into interendothelial clefts. Peroxidase does not traverse the endothelium of intramural arteries and arterioles of controls over the 10-minute period of observation. There is acceleration of lateral vesicular transport in the endothelium of epicardial arteries after angiotensin infusion and direct permeation of interendothelial clefts of intramural arterial vessels. Medial fragmentation and more extensive necrosis are observed in intramyocardial but not in epicardial arterial vessels. Foci of myocardial damage resembling irreversible ischemic or anoxic injury followed by reflow are described. It is suggested that the increased permeability of epicardial arteries may be due to elevated pressure, while the altered premeability and vascular lesions of intramural arteries and arterioles are more readily attributable to the vasoconstriction produced by angiotensin. The vascular and myocardial lesions are also discussed in relation to the regional actions of angiotensin on the coronary circulation and known effects of this vasoactive peptide on myocardium. (Am J Pathol 84:111–138, 1976)

THE ROLE OF RENIN or its active product, angiotensin II, in the pathogenesis of, and as a determinant for, the cardiovascular complications of the hypertensive state, is a matter of current interest and controversy. The debate stems from data suggesting that plasma renin levels are related to natural history and prognosis in essential hypertension.[1-3] Although other clinical studies appear to refute the hypothesis that hypertensive patients with elevated renin levels have an increased incidence of myocardial infarction and stroke,[4-8] the experimental administration of angiotensin to animals can result in myocardial necrosis without apparent coronary artery occlusion.[9]

There is general agreement that angiotensin II is a powerful pressor agent and arteriolar constrictor that acts directly on vascular smooth muscle (for review, see Buñag[10] and Regoli *et al.*[11]). The injection of angiotensin causes an increase in the permeability of arterial vessels[12-14]

From the Department of Pathology, New York Medical College, Valhalla, New York.
Supported in part by Grant HL-13742 from the US Public Health Service.
Accepted for publication March 2, 1976.
Address reprint requests to Dr. Filiberto Giacomelli, Department of Pathology, Laboratory of Experimental Pathology, New York Medical College, Basic Science Building, Valhalla, NY 10595.

through contraction of their endothelial cells.[14] Continuous infusion of angiotensin into rats provokes medial necrosis in small intestinal arteries.[15-18] Studies dealing with the effects of angiotensin infusion on regional blood flow and vascular resistance indicate that different vasculatures exhibit varying degrees of reactivity to the vasoactive peptide.[10] A recent investigation has shown that small coronary arteries respond differently than large epicardial coronary vessels when angiotensin is injected directly into the coronary vasculature.[19]

The purpose of the present study was to examine the effects of angiotensin infusion on the permeability and ultrastructure of both epicardial and intramyocardial arteries of rats. The results indicate that the observed increase in permeability of both types of vessels has a different ultrastructural basis. Vascular lesions are described in intramyocardial arteries and arterioles but not in epicardial arteries. Foci of cardiac injury consistent with myocardial infarction have also been noted after angiotensin infusion.

Materials and Methods

Eleven male Holtzman rats weighing 180 to 240 g were used in this study. The animals were anesthetized with intramuscular injections of Nembutal (sodium pentobarbital, Abbott Laboratories, North Chicago, Ill.), 4 mg 100 g body weight.

Six rats were infused via the left femoral vein with a solution of synthetic angiotensin amide (Hypertensin, Ciba Pharmaceutical Co., Summit, N.J.) for 4 hours. The angiotensin was dissolved in normal saline (33 μg ml) and administered at a constant rate of 1.7 μg min kg (i.e., 0.31 ml 100 g hr). Four of these animals were injected through the right femoral vein with horseradish peroxidase (HRP) (Type II, Sigma Chemical Co., St. Louis, Mo.) dissolved in normal saline to a final volume of 0.4 ml and in the amount of 15 mg 100 g body weight. The other two animals were injected intravenously with a carbon suspension (Pelikan CII 1431a, Gunther Wagner Co., Hanover, Germany) containing approximately 100 mg carbon ml in a dose of 0.1 ml 100 g body weight. The animals were injected with HRP 40 seconds, 90 seconds, 2 minutes, and 4 minutes, respectively, before the termination of the infusion, and then sacrificed. Carbon was administered 45 minutes before the end of the angiotensin infusion.

The heart was exposed, rapidly excised, immersed in a formaldehyde-glutaraldehyde mixture,[20] and the ventricles opened. Rings 2 to 3 mm wide were cut perpendicular to the long axis and through the full thickness of the ventricles. The epicardial arteries were identified on the surface of the left ventricle and trimmed into blocks under a dissecting microscope. Strips from the deeper layers of left ventricular myocardium were also prepared. The specimens were placed in fresh fixative for an additional 3 hours at room temperature. The tissues were then washed several times in 0.1 M phosphate buffer (pH 7.2) and stored overnight at 4 C.

Five animals served as controls and were infused with physiologic saline for 4 hours at the same rate and volume as in rats given angiotensin. Four of these rats were injected with HRP 40 seconds and 2, 4, and 10 minutes, respectively, before termination of the infusions and then immediately sacrificed. The fifth animal was sacrificed 45 minutes after receiving colloidal carbon. The hearts were excised, and blocks and strips of left ventricular myocardium were prepared and fixed as before.

Slices measuring 40 to 50 μ in thickness were cut with a Smith-Farquhar tissue chopper

from the blocks and strips of tissue obtained from animals injected with peroxidase, care being taken to section the epicardial vessels transversely. The slices were then incubated in a medium containing 10 ml of 0.05 M Tris HCl buffer (pH 7.6), 5 mg of 3,3'-diaminobenzidine tetrahydrochloride, and 0.1 ml of freshly prepared 1% hydrogen peroxide. Sections measuring 12 to 15 μ in thickness were also cut, incubated, mounted on glass slides, and examined by light microscopy in order to monitor the reaction.

All specimens were postfixed in phosphate-buffered 1% osmium tetroxide, dehydrated in a graded series of acetones and embedded in Araldite. Two micron-thick sections of the plastic-embedded material were examined by phase contrast microscopy to identify both the epicardial and smaller intramyocardial (or intramural) coronary arteries, as well as to assess the presence of vascular labeling by carbon.[21] Thin sections were cut with a diamond knife, stained with lead citrate and/or uranyl acetate, and examined with a Philips EM 200 or Siemens 101 electron microscope.

Systolic blood pressures were recorded both prior to and at intervals during the course of the infusions by an indirect method described previously.[22] The systolic pressure in control animals never exceeded 120 mm Hg and was usually in the range of 75 to 115 mm Hg. Maximal systolic pressure in rats infused with angiotensin was 175 mm Hg, and ranged between 130 to 150 mm Hg.

Results

Phase Contrast Observations

The administration of colloidal carbon to control animals and animals infused with angiotensin provides no evidence of vascular leakage. While intramyocardial arteries in angiotensin-treated rats exhibit irregular contours with a reduction in the diameters of their lumina and scalloping of adventitial surfaces, no appreciable constriction can be discerned in the epicardial arteries.

Ultrastructural Observations

Controls

The epicardial arteries possess an internal elastic lamella and several layers of smooth muscle cells with intervening plates of elastic tissue (Figure 1). Intramural arteries have an internal elastic lamella and one to three layers of medial smooth muscle cells (Figure 2). The smallest arterial vessels exhibit a single, sometimes incomplete, layer of smooth muscle, lack an internal elastic lamella, and have been considered arterioles.[23] Sarcomere-like arrays of filaments [24] that are aligned parallel to the longitudinal axis of the vessel are seen in both luminal and abluminal aspects of the endothelial cells lining intramural arteries and arterioles. Bundles of filaments are also present in the endothelium of epicardial arteries, but identification of a striated arrangement is precluded by the prior transverse orientation of the vessels.

At the earliest interval (40 seconds following HRP injection), most of the interendothelial cell clefts of epicardial arteries are devoid of tracer.

After 2 minutes, a reaction product may be found within segments of some clefts and a few contiguous pinocytotic vesicles (Figure 3). Small amounts of tracer can be present in the subendothelial space. After 4 minutes, HRP fills the entire length of interendothelial cell clefts and adjacent lateral vesicles and is also seen in both luminal and abluminal vesicles (Figure 4). The tracer extends into the subendothelial space and along basement membranes surrounding smooth muscle cells. The electron density of the reaction product within abluminal vesicles is similar to that seen in the subendothelial space but is less than the electron opacity of luminal vesicular contents. No instances are encountered where the vesicles are stained with HRP throughout endothelial cytoplasm (Figures 1, 3, and 4).

Horseradish peroxidase is not found in all of the lumina of intramyocardial arteries and arterioles. The vessels that contain HRP also exhibit reaction product in the luminal portions of interendothelial cell clefts and a few luminal vesicles (Figure 2). Neither permeation of the entire cleft nor distribution of HRP-laden vesicles throughout endothelial cell cytoplasm were seen during the 10-minute period of observation (Figures 2 and 5–8). Intramural arterial vessels not perfused by HRP are usually located near capillaries that contain reaction product. HRP extends from these capillaries into the interstitial tissue and penetrates through the walls of the arterial vessels into the subendothelial space (Figure 9). HRP is restricted to the abluminal segments of their intercellular endothelial clefts and only labels abluminal vesicles.

The fine structure of left ventricular myocardium of control animals conforms with previous descriptions of normal rat myocardium.[25]

Angiotensin-Infused Animals

As early as 40 seconds and no later than 90 seconds after the injection of HRP into hypertensive animals, epicardial arteries exhibit reaction product throughout the entire length of interendothelial cell clefts and adjacent subendothelial space (Figures 10 and 11). Many contiguous lateral vesicles contain HRP. A few HRP-labeled vesicles are seen at both luminal and abluminal surfaces of the endothelium. A rare interendothelial separation filled with HRP can also be found (Figure 12).

Within 90 seconds following the administration of HRP to angiotensin-infused rats, reaction product fills entire interendothelial cell clefts of intramyocardial arteries and arterioles, the direction of permeation being either from the luminal (Figure 13) or abluminal (Figure 14) ends of the clefts. There is an increase in the number of labeled endothelial vesicles over the 4-minute period of examination, but they are essentially re-

stricted to either luminal or abluminal portions of endothelial cytoplasm, depending upon the direction of permeation (Figure 15).

Particles of colloidal carbon are not found within the walls of arterial vessels or extravascular tissues from hypertensive animals.

While the epicardial arteries do not show appreciable morphologic changes following angiotensin infusion, prominent alterations occur in the walls of intramyocardial arteries and arterioles. Contraction of medial smooth muscle cells is manifested by variation in the size and shape of these cells and marked scalloping of their adventitial surfaces (Figures 16 and 17). The luminal surface of the endothelium is irregular, with infolding of the internal elastic lamella and bulging of endothelial cells into narrowed lumina. Numerous invaginations of endothelial and smooth muscle cell nuclei are also seen (Figure 17). Focal areas are observed, primarily in intramural arteries and occasionally in arterioles, where the media is occupied by fragments of smooth muscle cells of variable size (Figures 16, 18 and 19). The spaces between the muscle cell fragments in vessels from animals injected with HRP are permeated by the tracer in many instances (Figures 16 and 18). An occasional muscle cell fragment exhibits lysis, with vacuolization and loss of cytoplasmic organelles (Figure 19). A variety of tubulovesicular debris and electron-dense granules may be distributed extracellularly around such fragments. Penetration of intramyocardial arterial vessel walls by HRP is seen in vessels with and without medial lesions.

More extensive areas of injury are also seen in the walls of constricted small arteries and arterioles (Figures 20 and 21), involving either a portion or the entire circumference of a vessel in transverse section. The nuclei of endothelial and smooth muscle cells exhibit either pyknosis or rarefaction, with peripheral clumping of chromatin. There is loss of myofilaments from smooth muscle cell cytoplasm, and clusters of thick filaments measuring 150 to 170 Å in diameter are visible. Large electron-lucent vacuoles are also seen in endothelial and smooth muscle cell cytoplasm (Figures 21 and 22). The lumina of these vessels are generally devoid of HRP but may contain closely packed erythrocytes, membrane-limited bodies, and a few platelets. A rare platelet plug within unaltered arterioles can also be found (Figure 23).

Foci of damage are present in the myocardium. In such areas, there is peripheral clumping of nuclear chromatin in the myocytes and loss of glycogen from myofibrils (Figure 22). The myofibrils show varying degrees of contraction with the formation of contraction zones and/or bands (Figures 22 and 24–26). Large aggregates of mitochondria are packed between contractile elements (Figure 22). The mitochondria are swollen,

have a decreased matrix density and lesser numbers of cristae, exhibit partial-to-total absence of matrix granules, and possess variable numbers of larger amorphous matrix densities (Figures 24 and 26). Electron-dense material may be present within cristal membranes (Figure 24). The sarcoplasmic reticulum and T-system show varying degrees of dilatation, and there may even be vacuolization of the sacroplasmic reticulum. There is prominent invagination of the sarcolemma in register with the underlying contraction zones (Figure 25). Numerous vacuoles are observed beneath the sarcolemma (Figure 26). There may also be tearing and detachment of the plasmalemma from adjacent basement membranes.

Polymorphonuclear neutrophilic leukocytes, erythrocytes, and macrophages are seen outside venules in some lesions (Figure 27). The myofibrils lack the usual striated arrangement and exhibit severe vacuolization of translocated mitochondria and a variety of cellular debris (Figures 27 and 28).

The intercalated discs between hypercontracted myofibers run an extremely tortuous course (Figure 22), with nonspecialized contact zones poorly defined, and the fasciae adherentes fragmented (Figure 20) and irregularly distributed (Figures 29 and 30). The regions of the desmosomal contacts and gap junctions are unaltered (Figure 30). Foci are noted where myofilaments are enclosed within membranes of the intercalated disc proper (Figure 30). While myofilaments have pulled away from the intercalated disc in one myofiber, they may remain attached in the adjacent and seemingly more contracted myofiber (Figures 22 and 29).

No definite topographic relationship can be established in any single plane of section between foci of myocardial injury and intramural arterial lesions.

Discussion

The present observations indicate that large epicardial and small intramyocardial arteries and arterioles of control rats differ with respect to their permeability to macromolecules such as HRP (molecular weight approximately 40,000). After 4 minutes, HRP penetrates the interendothelial clefts of epicardial arteries via lateral pinocytotic vesicles that appear to circumvent intercellular endothelial junctions. In contrast, the probe molecule does not traverse the endothelium lining intramural arteries and arterioles over the 10-minute period of observation, HRP invariably being arrested within the clefts at the level of the interendothelial junctions. Transvascular passage of the tracer is markedly accelerated in the vessels from animals with acute hypertension. Vesicular discharge into the clefts of epicardial arteries and permeation of the subendothelial space

occur as early as 40 seconds. Within 90 seconds of the injection of HRP, there is a bidirectional flux of tracer through the entire length of interendothelial clefts of intramural arteries and arterioles.

The conclusion that HRP does not enter the subendothelial space of epicardial arteries of control animals by directly permeating interendothelial clefts is based upon the observation that reaction product is initially restricted to segments of clefts that communicate with lateral vesicles containing HRP, suggesting that these portions of the clefts have been filled by the discharge of parajunctional vesicles. A similar mechanism has been postulated for the passage of HRP across aortic endothelium.[26,27] This process is more apparent in the epicardial arteries of the hypertensive animals. However, the possibility that the labeling of parajunctional vesicles represents uptake of HRP from the clefts cannot be entirely excluded. The small number and restriction of HRP-labeled vesicles to luminal and/or abluminal portions of the endothelium of epicardial arteries strongly suggests that there is no significant vesicular transport directly across the endothelium of these vessels, the apparent filling of such vesicles representing communication with lumen or subendothelial space. However, direct vesicular transport across arterial endothelium can be increased in experimental hypertension.[28-30] The occurrence of rare interendothelial separations furnishes an additional mechanism to account for the increased permeability of the larger coronary vessels in acute hypertension.

While the infusion of angiotensin accelerates normal transport in epicardial arteries, it causes a breach in the barrier previously constituted by interendothelial cell junctions of intramural arteries and arterioles. An increase in vascular permeability and separation of intercellular endothelial junctions of mesenteric arteries have previously been described in acute angiotensin-induced hypertension in the rat,[15-17] as well as in the arterial vessels of animals with other forms of experimental hypertension.[30,31] Intraarterial injection of angiotensin II can also produce intercellular endothelial separations.[12,14] The increase in the permeability of the aorta and major coronary arteries that follows upon intracardiac injection of angiotensin is associated with the formation of interendothelial gaps that have been related to endothelial cell contraction.[14]

The difference in the permeability properties of epicardial vs. intramyocardial arteries and arterioles from control and angiotensin-infused rats reflects regional variation in the permeability pathways across arterial endothelium. The fact that permeability differences exist within the same circulation has a precedence in the aorta, where different areas (ostial vs. interostial) show a variation in permeability that has been ascribed to

hemodynamic phenomena.[27] The coronary artery system consists of two functionally different segments of vessels. The larger and superficial epicardial arteries are conduit channels that respond passively to significant modifications in intraarterial pressure, while the smaller intramural arteries tend to autoregulate and maintain constant flow by dilatation or constriction.[19,32] Blood flow in an organ is mainly determined by the perfusion pressure and vascular resistance, and the coronary vessels uniquely have their caliber (particularly that of intramural vessels) affected by mechanical compression from contracting myocardial fibers. While epicardial arteries are exposed to both systolic and diastolic perfusion pressures, the intramyocardial arteries are primarily perfused during the diastolic phase of the cardiac cycle.[33,34] Thus, epicardial arteries in angiotensin-infused animals could be exposed to both mechanical effects and the vasoconstrictor action of angiotensin, while intramural arteries and arterioles that are protected from the elevated systolic pressure would be exposed primarily to angiotensin effects. Since the caliber and ultrastructure of the epicardial arteries do not appear to be altered by angiotensin infusion, it seems more likely that their increased permeability could be the result of elevated perfusion pressure rather than an angiotensin effect. In contrast, intramyocardial arteries and arterioles exhibit increased permeability and morphologic alterations that could represent a response to the vasoconstrictor action of angiotensin II. However, the possibility that the elevated perfusion (diastolic) pressure plays a role in the increased permeability of intramural vessels cannot be excluded.

One factor promoting the breach in the interendothelial cell junctions of intramural arteries and arterioles may be focal weakening in the walls caused by the fragmentation of medial smooth muscle cells. The latter change could represent the morphologic basis for the escape of intramyocardial arteries and arterioles from the vasoconstrictor or autoregulatory phenomena associated with angiotensin infusion.[19] This could also account for the increase in coronary flow that has been reported in anesthetized rats following angiotensin administration.[35-37]

Another factor affecting the permeability of intramural arteries and arterioles could be the angiotensin-mediated contraction of endothelial cells that would tend to separate interendothelial junctions.[16] Angiotensin acts directly on the blood vessel wall, binding to endothelial surface membranes [38] or nuclei of endothelial and smooth muscle cells.[39] Specific angiotensin receptors have also been demonstrated in a microsomal fraction of smooth muscle, and displacement of calcium ions from microsomal particles follows angiotensin–receptor interaction.[40,41] The resultant increase in calcium concentration may account for the contraction of myo-

filaments. The bundles of filaments observed in coronary artery endothelium of both control and hypertensive animals could be the morphologic counterparts of contractile proteins.[42,43]

There is a bidirectional flux of HRP from lumen or subendothelial space into the interendothelial clefts of intramural arteries and arterioles of control animals, the gradient between perfusion pressure and tissue pressure at any point in time determining the direction of diffusion. Retrograde filling of the clefts by HRP from the perivascular space occurs in vessels that have not been perfused by the tracer, the probe molecule having diffused through the interstitium from adjacent peremeated capillaries.[44] Thus, reverse filling of the clefts in control animals may be the result of a "milking" effect of myocardial contraction on unperfused arterial vessels. This bidirectional flux of HRP persists in animals infused with angiotensin II. There is, however, complete penetration of the clefts in this case. The factor promoting permeation of interendothelial cell junctions of intramyocardial arteries and arterioles of hypertensive animals could once again be angiotensin-mediated endothelial cell contraction.[16]

The acute hypertension that follows the infusion of angiotensin II is associated with two types of ultrastructural alterations that are limited entirely to intramural arteries and arterioles. The more frequent alteration consists of the focal fragmentation of severely contracted medial smooth muscle cells. Smooth muscle cell fragmentation has previously been observed in mesenteric arteries of rats with angiotensin-induced hypertension,[15-18] where it has been associated with endothelial discontinuities and insudation of plasma proteins, fibrin, platelets, and intravenously injected colloidal carbon particles. These medial changes have been attributed to either sustained contraction beyond the metabolic capability of the smooth muscle cells [16] or to the insudation of plasma constituents through endothelial discontinuities.[15] The fact that medial fragmentation may occur in the coronary vasculature without endothelial discontinuities or frank insudative phenomena supports the prior suggestion regarding the primacy of medial alterations in angiotensin-induced hypertension.[16] The absence of frank interendothelial separations and intramural accumulation of fibrin, platelets, and colloidal carbon in small coronary arteries and arterioles may be related to the protection of these vessels from the mechanical effects of elevated systolic pressure provided by myocardial contraction.

The second and less frequent alteration in the ultrastructure of intramyocardial arteries and arterioles involves the full thickness of the vessel walls, with both endothelial and smooth muscle cells exhibiting

nuclear and cytoplasmic swelling and lysis. The lumina of such vessels are generally narrowed, do not contain peroxidase, and are packed with red blood cells, membrane-limited bodies, or platelets. These observations suggest that the circulation through the intramural vessels is impaired and that the vascular degeneration may have an ischemic or anoxic basis. Membrane-limited bodies have previously been found in capillaries associated with the "no-reflow" phenomenon following cerebral [45] and myocardial [46] ischemia. These structures are thought to originate as blebs from damaged endothelium and/or platelets. Such bodies could also represent red blood cell ghosts. Ischemia followed by reperfusion can result in swelling and degeneration of endothelial and smooth muscle cells.[47] There is some evidence from previous work, as well as from the present study, that the intravascular injection of angiotensin II can produce temporary platelet aggregation and adherence to arterial endothelium.[14,48] Angiotensin II has been reported to potentiate the action of adrenalin or adenosine diphosphate on platelets *in vitro*.[49] Alternatively, the intravascular accumulation of hematologic elements may be secondary to the observed myocardial lesions, an explanation previously offered for the coronary thrombi associated with acute myocardial infarction in man.[50]

Foci of myocardial injury characterized by contraction zones; abnormalities of the sarcoplasmic reticulum, mitochondria, and nuclei; and alterations in the intercalated discs have been observed in areas that have no consistent topographic relationship to intramyocardial arteries and arterioles. On the whole, these morphologic changes resemble the alterations associated with irreversible myocardial injury and reflow after ischemic [51] or anoxic [52] episodes and could therefore be the result of either temporary coronary arterial occlusion or a relative anoxia due to increased cardiac energy requirements produced either directly or indirectly by angiotensin II. Angiotensin has been reported to enhance myocardial contraction by facilitating the entry of calcium ions into myocardial fibers. However, there are some data indicating that the positive inotropic action of angiotensin may be due to endogenous catecholamine release (for discussion see Buñag [10] and Dempsey and Cooper [53]). Excessive endogenous secretion or the exogenous administration of catecholamines can produce myocardial necrosis.[54-56] An additional effect of catecholamine release on the induction or development of myocardial necrosis could be the synergistic action of angiotensin II and epinephrine on platelet aggregation.[49] The myocardial necrosis and hypercontraction resulting from isoproterenol administration has been attributed to massive calcium influx into the myofibers.[57]

Areas are noted within myocardium where there is considerable dis-

sociation of myofibrillar insertions into intercalated discs. The intercalated discs run an irregular course and display separations of variable extent. The integrity of the intercalated disc varies considerably in the oxygen-deficient heart under different experimental conditions. Although the intercalated disc of dog heart has appeared normal after coronary artery occlusion for 40 minutes,[51] other workers have described separations of the discs in such animals 8 days after acute coronary artery occlusion.[58] Normothermic ischemic arrest of the dog heart results in dissolution of the specialized portions of the discs.[59] Both acute [60,61] and chronic hypoxia [62] cause variable degrees of dissociation in the discs of rat myocardium. For reasons just described the continuous infusion of angiotensin II could result in periods of ischemia and/or hypoxia that could weaken intercalated discs.

Little is known about the mechanisms involved in the dehiscence of the intercalated disc and its myofibrillar insertions. It seems likely to be related to the pulling force applied to weakened intercellular contacts.[63] The forces generated by overcontraction of myofibrils in either a single or pair of apposing cells could represent the structural basis for the disc changes observed in the present study. At times the intercalated discs enclose bundles of myofilaments from adjacent myofibrils, an alteration previously ascribed to displacement or herniation in hypovolemic shock.[64] Isoproterenol-induced myocardial necrosis is also associated with hypercontraction of myofilaments and herniation of intercalated discs.[65]

The concept that renin, or more strictly its active product angiotensin II, may cause vascular lesions in hypertension is not novel. Studies designed to explore the role of the renin–angiotensin system in the genesis of hypertensive vascular disease have been difficult to interpret since it has been impossible to discriminate direct renin–angiotensin effects from those associated with the elevation in systemic pressure. Examination of the differential response of the coronary artery system to angiotensin infusion has provided additional information in this regard. While the increase in permeability of the larger epicardial arteries appears to be related to the mechanical effects of elevated pressure, the increase in permeability and vascular lesions in the smaller intramyocardial arteries and arterioles are more readily attributable to the vasoconstriction provoked by angiotensin II. Although the actual mechanism by which hypertension accelerates atherosclerosis has not been established, additional evidence is provided by the present study that hypertension may further augment the endothelial permeability associated with atherosclerosis [66–69] and that vasoactive agents such as angiotensin may mediate this phenomenon by exaggerating physiologic transport across arterial endothelium.

The occurrence of myocardial lesions with an ultrastructure compatible with myocardial infarction following angiotensin infusion may also be relevant to the problem of renin as a risk factor for cardiovascular complications in essential hypertension. Clinical studies regarding the prevalence of myocardial infarction and strokes in high vs normal and low renin hypertensive subjects have provided contradictory data.[1-8] However, there can be no doubt that the experimental administration of renin or angiotensin can produce myocardial necrosis and/or infarction in animals. In addition to the well-recognized vasoactive properties of angiotensin II, the cardiotoxic potential of this peptide also merits serious consideration.

References

1. Brunner HR, Laragh JH, Baer L, Newton MA, Goodwin FT, Krakoff LR, Bard RH, Buhler FR: Essential hypertension: Renin and aldosterone, heart attack and stroke. N Engl J Med 286:441–449, 1972
2. Weinberger MH, Yu PL, Perkins BJ: Renin in hypertension: Further evidence for a vasculotoxic role. Clin Res 21:458, 1973 (Abstr)
3. Christlieb AR, Gleason RE, Hickler RB, Lauler DP: Renin: A risk factor for cardiovascular disease? Ann Intern Med 81:7–10, 1974
4. Doyle AE, Jerums G, Johnston CI, Louis WJ: Plasma renin levels and vascular complications in hypertension. Br Med J 2:206–207, 1973
5. Genest J, Boucher R, Kuchel O, Nowaczynski W: Renin in hypertension: How important as a risk factor? Can Med Assoc J 109:475–478, 1973
6. Gulati SC, Adlin EV, Biddle CM, Marks AD, Channick BJ: The occurrence of vascular complications in low renin hypertension. Ann Intern Med 78:828, 1973 (Abstr)
7. Mroczek WJ, Finnerty FA, Catt KJ: Lack of association between plasma-renin and history of heart-attack or stroke in patients with essential hypertension. Lancet 2:464–469, 1973
8. Stroobandt R, Fagard R, Amery AKPC: Are patients with essential hypertension and low renin protected against stroke and heart attack? Am Heart J 86:781–787, 1973
9. Gavras H, Brown JJ, Lever AF, Macadam RF, Robertson JIS: Acute renal failure, tubular necrosis, and myocardial infarction induced in the rabbit by intravenous angiotensin II. Lancet 2:19–22, 1971
10. Buñag RD: Circulatory effects of angiotensin. Handbook of Experimental Pharmacology. Edited by IH Page, FM Bumpus. New York, Springer-Verlag, 1974, pp 441–454
11. Regoli D, Park WK, Rioux F: Pharmacology of angiotensin. Pharmacol Rev 26:69–123, 1974
12. Constantinides P, Robinson M: Ultrastructural injury of arterial endothelium. II. Effects of vasoactive amines. Arch Pathol 88:106–112, 1969
13. Robertson AL, Khairallah PA: Effects of angiotensin II and some analogues on vascular permeability in the rabbit. Circ Res 31:923–931, 1972
14. Robertson AL Jr, Khairallah PA: Arterial endothelial permeability and vascular disease: The "trap door" effect. Exp Mol Pathol 18:241–260, 1973
15. Goldby FS, Beilin LJ: How an acute rise in arterial pressure damages arterioles: Electron microscopic changes during angiotensin infusion. Cardiovasc Res 6:569–584, 1972

16. Wiener J, Giacomelli F: The cellular pathology of experimental hypertension. VII. Structure and permeability of the mesenteric vasculature in angiotensin-induced hypertension. Am J Pathol 72:221–240, 1973
17. Thorball N, Olsen F: The permeability pathways in the walls of intestinal submucosal arterioles in acute angiotensin-induced hypertension in rats. Acta Pathol Microbiol Scand [A] 82:683–689, 1974
18. Thorball N, Olsen F: Ultrastructural pathological changes in intestinal submucosal arterioles in angiotensin-induced acute hypertension in rats. Acta Pathol Microbiol Scand [A] 82:703–713, 1974
19. Cohen MV, Kirk ES: Differential response of large and small coronary arteries to nitroglycerin and angiotensin: Autoregulation and tachyphylaxis. Circ Res 33:445–453, 1973
20. Graham RC Jr, Karnovsky MJ: The early stages of absorption of injected horseradish peroxidase in the proximal tubules of mouse kidney: Ultrastructural cytochemistry by a new technique. J Histochem Cytochem 14:291–302, 1966
21. Majno G, Palade GE, Schoefl GI: Studies on inflammation. II. The site of action of histamine and serotonin along the vascular tree: A topographic study. J Biophys Biochem Cytol 11:607–626, 1961
22. Spiro D, Lattes RG, Wiener J: The cellular pathology of experimental hypertension. I. Hyperplastic arteriolarsclerosis. Am J Pathol 47:19–49, 1965
23. Wiener J, Spiro D, Lattes RG: The cellular pathology of experimental hypertension. II. Arteriolar hyalinosis and fibrinoid change. Am J Pathol 47:457–485, 1965
24. Giacomelli F, Wiener J, Spiro D: Cross-striated arrays of filaments in endothelium. J Cell Biol 45:188–192, 1970
25. Stenger RJ, Spiro D: The ultrastructure of mammalian cardiac muscle. J Biophys Biochem Cytol 9:325–351, 1961
26. Schwartz SM, Benditt EP: Studies on aortic intima. I. Structure and permeability of rat thoracic aortic intima. Am J Pathol 66:241–264, 1972
27. Giacomelli F, Wiener J: Regional variation in the permeability of rat thoracic aorta. Am J Pathol 75:513–528, 1974
28. Hüttner I, More RH, Rona G: Fine structural evidence of specific mechanism for increased endothelial permeability in experimental hypertension. Am J Pathol 61:395–412, 1970
29. Giacomelli F, Wiener J, Spiro D: The cellular pathology of experimental hypertension. V. Increased permeability of cerebral arterial vessels. Am J Pathol 59:133–160, 1970
30. Suzuki K, Ooneda G: Cerebral arterial lesions in experimental hypertensive rats: Electron microscopic study of middle cerebral arteries. Exp Mol Pathol 16:341–352, 1972
31. Wiener J, Lattes RG, Meltzer BG, Spiro D: The cellular pathology of experimental hypertension. IV. Evidence for increased vascular permeability. Am J Pathol 54:187–207, 1969
32. Fam WM, McGregor M: Effect of nitroglycerin and dipyridamole on regional coronary resistance. Circ Res 22:649–659, 1968
33. Kirk ES, Honig CR: An experimental and theoretical analysis of myocardial tissue pressure. Am J Physiol 207:361–367, 1964
34. Gregg DE, Khouri EM, Rayford CR: Systemic and coronary energetics in the resting unanesthetized dog. Circ Res 16:102–113,, 1965
35. Gömöri P, Takács L, Kállay K: The effect of synthetic angiotensin II on the redistribution and shifting of blood. Arch Int Pharmacodyn Ther 138:254–262, 1962
36. Mandel MJ, Sapirstein LA: Effect of angiotensin infusion on regional blood flow and regional vascular resistance in the rat. Circ Res 10:807–816, 1962

37. Kapitola J, Kūchel O, Schreiberová O, Jahoda I: Blood flow through organs of the rat after an intravenous injection of angiotensin. Physiol Bohemoslov 17:437–443, 1968
38. Richardson JB, Beaulnes A: The cellular site of action of angiotensin. J Cell Biol 51:419–432, 1971
39. Robertson AL Jr, Khairallah PA: Angiotensin II: Rapid localization in nuclei of smooth and cardiac muscle. Science 172:1138–1139, 1971
40. Baudouin M, Meyer P, Fermandjian S, Morgat J-L: Calcium release induced by interaction of angiotensin with its receptors in smooth muscle cell microsomes. Nature (Lond) 235:336–338, 1972
41. D'Auriac GA, Baudouin M, Meyer P: Mechanism of action of angiotensin in smooth muscle cell: Biochemical changes following interaction of the hormone with its membrane receptors. Circ Res 30-31(Suppl 2):II151–II160, 1972
42. Becker CG, Murphy GE: Demonstration of contractile protein in endothelium and cells of the heart valves, endocardium, intima, arteriosclerotic plaques, and Aschoff bodies of rheumatic heart disease. Am J Pathol 55:1–38, 1969
43. Yohro T, Burnstock G: Filament bundles and contractility of endothelial cells in coronary arteries. Z Zellforsch Mikrosk Anat 138:85–95, 1973
44. Karnovsky MJ: The ultrastructural basis of capillary permeability studied with peroxidase as a tracer. J Cell Biol 35:213–236, 1967
45. Chiang J, Kowada M, Ames A III, Wright RL, Majno G: Cerebral ischemia. III. Vascular changes. Am J Pathol 52:455–476, 1968
46. Kloner RA, Ganote CE, Jennings RB: The "no-reflow" phenomenon after temporary coronary occlusion in the dog. J Clin Invest 54:1496–1508, 1974
47. Elemér G, Kerényi T, Jellinek H: Effect of temporary hypoxia on the permeability of the rat aorta. Pathol Eur 10:123–128, 1975
48. Kincaid-Smith P, Hobbs JB, Friedman A, Mathews DC: Structural and ultrastructural alterations in mesenteric and renal arterioles following infusion of vaso-active agents. Hypertension '72. Edited by J Genest, E Koiw. New York, Springer-Verlag, 1972, pp 97–108
49. Poplawski A: Effect of angiotensin II on the platelet aggregation induced by adenosine-diphosphate, epinephrine and thrombin. Experientia 26:86, 1969
50. Roberts WC, Buja LM: The frequency and significance of coronary arterial thrombi and other observations in fatal acute myocardial infarction: A study of 107 necropsy patients. Am J Med 52:425–443, 1972
51. Herdson PB, Sommers HM, Jennings RB: A comparative study of the fine structure of normal and ischemic dog myocardium with special reference to early changes following temporary occlusion of a coronary artery. Am J Pathol 46:367–386, 1965
52. Ganote CE, Seabra-Gomes R, Nayler WG, Jennings RB: Irreversible myocardial injury in anoxic perfused rat hearts. Am J Pathol 80:419–450, 1975
53. Dempsey PJ, Cooper T: Pharmacology of the coronary circulation. Annu Rev Pharmacol 12:99–110, 1972
54. Szakács JE, Cannon A: l-Norepinephrine myocarditis. Am J Clin Pathol 30:425–434, 1958
55. Szakács JE, Mehlman B: Pathologic changes induced by l-norepinephrine: Quantitative aspects. Am J Cardiol 5:619–627, 1960
56. Ferrans VJ, Hibbs RG, Black WC, Weilbaecher DG: Isoproterenol-induced myocardial necrosis. A histochemical and electron microscopic study. Am Heart J 68:71–90, 1964
57. Bloom S, Davis DL: Calcium as mediator of isoproterenol-induced myocardial necrosis. Am J Pathol 69:459–470, 1972
58. Schwartz A, Wood JM, Allen JC, Bornet EP, Entman ML, Goldstein MA, Sordahl LA, Suzuki M: Biochemical and morphologic correlates of cardiac ischemia. I. Membrane systems. Am J Cardiol 32:46–61, 1973

59. McCallister LP, Munger BL, Tyers GFO, Hughes HC: The effect of different methods of protecting the myocardium on lysosomal activation and acid phosphatase activity in the dog heart after one hour of cardiopulmonary bypass. J Thorac Cardiovasc Surg 69:644–663, 1975
60. Büchner F, Onishi S: Frühstadien der akuten hypoxischen Veränderung des Herzmuskels im elektronenmikroskopischen Bild und ihre Bedeutung für die akute hypoxische Herzinsuffizienz. Beitr Pathol Anat 135:153–182, 1967
61. Büchner F, Onishi S: Der Herzmuskel bei akuter Koronarinsuffizienz im elektronenmikroskopischen Bild. Munich, Urban and Schwarzenberg, 1968, pp 60–65
62. Sulkin NM, Sulkin DF: An electron microscopic study of the effects of chronic hypoxia on cardiac muscle, hepatic, and autonomic ganglion cells. Lab Invest 14:1523–1546, 1965
63. Kawamura K, James TN: Comparative ultrastructure of cellular junctions in working myocardium and the conduction system under normal and pathologic conditions. J Mol Cell Cardiol 3:31–60, 1971
64. Unger SW, Ratliff NB: The relationship of actin and myosin filaments within myocardial zonal lesions. Am J Pathol 80:471–480, 1975
65. Csapó Z, Dusek J, Rona G: Peculiar myofilament changes near the intercalated disc in isoproterenol-induced cardiac muscle cell injury. J Mol Cell Cardiol 6:79–83, 1974
66. Friedman M, Byers SO: Endothelial permeability in atherosclerosis. Arch Pathol 76:99–105, 1963
67. Stefanovich V, Gore I: Cholesterol diet and permeability of rabbit aorta. Exp Mol Pathol 14:20–29, 1971
68. Pries C, Klynstra FB: Aortic permeability, lipids, and atherosclerosis. Lancet 1:750–751, 1971
69. Bondjers G, Björkerud S: Cholesterol accumulation and content in regions with defined endothelial integrity in the normal rabbit aorta. Atherosclerosis 17:71–83, 1973

Acknowledgments

The authors wish to acknowledge with thanks the technical assistance of Maria Demeri and Georganne Hoffman. The photographic contributions of Alfred E. Revzin are greatly appreciated.

[*Illustrations follow*]

Legends for Figures

Figures 1-9 are electron micrographs of coronary arteries from control animals.

Figure 1—Epicardial artery from animal injected with HRP 4 minutes prior to sacrifice. Fenestrated plates of elastic tissue are interposed between the endothelium and medial smooth muscle cells as well as between the layers of smooth muscle cells. Peroxidase is seen on the luminal surface of the endothelium and within luminal pinocytotic vesicles. The tracer also fills the luminal portions of interendothelial clefts (*arrows*). Although there is some peroxidase in the subendothelial space, vesicles are not labeled throughout endothelial cytoplasm. *L* = lumen. (× 6000).

Figure 2—The lumen of this intramyocardial artery contains erythrocytes and peroxidase. The tracer is restricted to luminal endothelial vesicles and luminal segments of intercellular endothelial clefts. HRP injected 40 seconds previously. (× 9500)

Figure 3—Horseradish peroxidase is seen in a segment of interendothelial cleft and contiguous vesicles of epicardial artery 2 minutes after the injection of peroxidase. There is slight staining of the subendothelial space by the tracer. *L* = lumen. (× 35,500)

Figure 4—Peroxidase is seen on the luminal surface and throughout the interendothelial cleft of an epicardial artery 4 minutes after injection of the tracer. Several lateral endothelial vesicles and the subendothelial space also contain HRP. Other vesicles distributed through the endothelial cytoplasm are not labeled by the tracer. *L* = lumen. (× 26,000)

Figures 5-8—Interendothelial clefts of intramural arteries 40 seconds (**5**), 2 minutes (**6**), 4 minutes (**7**), and 10 minutes (**8**) after the injection of peroxidase. HRP is arrested within the clefts. There is also staining of the subendothelial space by tracer that has extended from adjacent capillaries (see text). *L* = lumen. (**5**, × 26,000; **6**. × 30,500; **7**. × 31,500; **8**. × 41,500)

Figure 9—Reverse permeation of the wall of an intramyocardial artery 10 minutes after injection of HRP. Note that the lumen is devoid of tracer. There is heavy staining of the basement membranes around the smooth muscle cells and extension into the subendothelial space and adjacent segments of intercellular endothelial clefts. Abluminal vesicles also contain peroxidase. The interendothelial junction indicated by the *arrow* is shown at higher magnification in the inset. (× 7500) **Inset**—HRP is seen within the subendothelial space, the adjacent basal segment of the cleft, as well as in a few abluminal vesicles. *L* = lumen. (× 29,500)

Figures 10-30 are electron micrographs of arterial vessels and myocardium from animals infused with angiotensin.

Figure 10—Reaction product is seen within an interendothelial cleft and adjoining vesicles of an epicardial artery 40 seconds after HRP injection. *L* = lumen. (× 30,500)

Figure 11—Similar to Figure 10. There is a considerable amount of HRP in the adjacent subendothelial space 90 seconds after injection of the probe molecule. *L* = lumen. (× 25,000)

Figure 12—Interendothelial separation of epicardial artery is filled with peroxidase that has been injected 40 seconds previously. Reaction product is also seen within the subendothelial space and along the basement membrane investing a smooth muscle cell (*S*). *L* = lumen. (× 33,000)

Figure 13—Peroxidase is found within an intercellular endothelial cleft, luminal vesicles, and subendothelial space of intramural artery 90 seconds after HRP injection. Note the gradient in the electron density of the reaction product from lumen to subendothelium. *L* = lumen. (× 30,000)

Figure 14—Interendothelial cleft of an intramural arteriole is permeated by peroxidase that has extended from the subendothelial space. There is also filling of abluminal vesicles (*V*). HRP was injected 90 seconds previously. *L* = lumen. (× 30,000)

Figure 15—Only the luminal endothelial vesicles of an intramural artery are heavily labeled with peroxidase after 2 minutes. One interendothelial cleft (*arrow*) is entirely permeated. There is also staining of the subendothelium and abluminal vesicles. Note that the pinocytotic vesicles in the intermediate portions of the endothelium do not contain HRP. (× 15,000)

Figure 16—Contraction of the muscle cells of an intramyocardial artery is manifested by scalloping of the adventitial surface. Note the foci of medial fragmentation (*brackets*). (× 8000)

Figure 17—Scalloping of the adventitial surface of an intramural arteriole is readily apparent. There are numerous indentations of an endothelial nucleus (*N*). (× 8000)

Figure 18—Medial fragmentation of the smooth muscle cells of an intramural artery. The extracellular space between the fragments is heavily labeled by peroxidase. (× 6500)

Figure 19—Medial fragmentation of intramyocardial artery from animal injected with carbon. A few fragments are undergoing lysis (*arrows*). A variety of tubulovesicular and granular debris are present in the media and are seen to better advantage in the absence of peroxidase. Note the striated array of filaments at the luminal endothelial surface (*interrupted arrows*). (× 15,500)

Figures 20 and 21—Different levels of the same intramyocardial artery. The lumina are filled with membrane-limited bodies and/or an erythrocyte. There is rarefaction of endothelial and smooth muscle cell nuclei and loss of myofilaments. A large endothelial vacuole (*V*) is also present (**21**). (× 5000)

Figure 22—Montage containing arteriole and three adjacent myofibers. The lumen of the arteriole contains red cells, platelets, and endothelial blebs (*B*). Large vacuoles are also seen in the smooth muscle cells (*V*).There is loss, as well as clumping, of endothelial and smooth muscle cell nuclear chromatin. Numerous contraction zones are seen in the central myofiber. There is aggregation and packing of mitochondria between the myofibrils and clumping of nuclear chromatin. The other two fibers exhibit less extensive contraction of sarcomeres and aggregation of mitochondria. The intercalated disc (*I*) of the central myofiber has a convoluted course. Note the separation of myofilaments on the other side of this disc. (× 3500)

Figure 23—A platelet plug fills the lumen of this arteriole (× 3000).

Figure 24—Aggregates of mitochondria containing large amorphous granules, decreased matrix density, and fewer numbers of cristae. Electron-dense material (*arrows*) is visible within some cristae. Contraction bands are present in the right lower corner of the micrograph. (× 26,500)

Figure 25—The scalloping of the sarcolemma lies in register with the underlying contraction zone (× 21,500).

Figure 26—There is detachment of plasmalemma from the basement membrane (*BM*). Subsarcolemmal vacuoles are also present. The mitochondria resemble those described in Figure 24. (× 18,500)

Figure 27—A polymorphonuclear neutrophilic leukocyte (*P*) lies outside a venule (*Ve*). There is swelling of mitochondria and accumulation of debris within the neighboring myofiber. (× 16,000)

Figure 28—The myofibrils lack their usual striated pattern. There is merging and fusion of adjacent Z lines to form contraction bands. Note the prominent vacuolization of mitochondria. (× 12,500)

Figure 29—Intercalated disc and adjacent myofibers. The fasciae adhaerentes are fragmented and distributed irregularly. The filaments in the upper myofiber have separated from the intercalated disc. The fiber on the other side of the disc exhibits contraction zones. (× 21,500)

Figure 30—Myofilaments of the upper fiber are enclosed by convolutions of the intercalated disc (*asterisks*). The fasciae adhaerentes are distributed irregularly once again. The gap junctions (G_1 and G_2) are unaltered. (× 13,000) **Inset**—G_1 is shown at higher magnification (× 65,000).

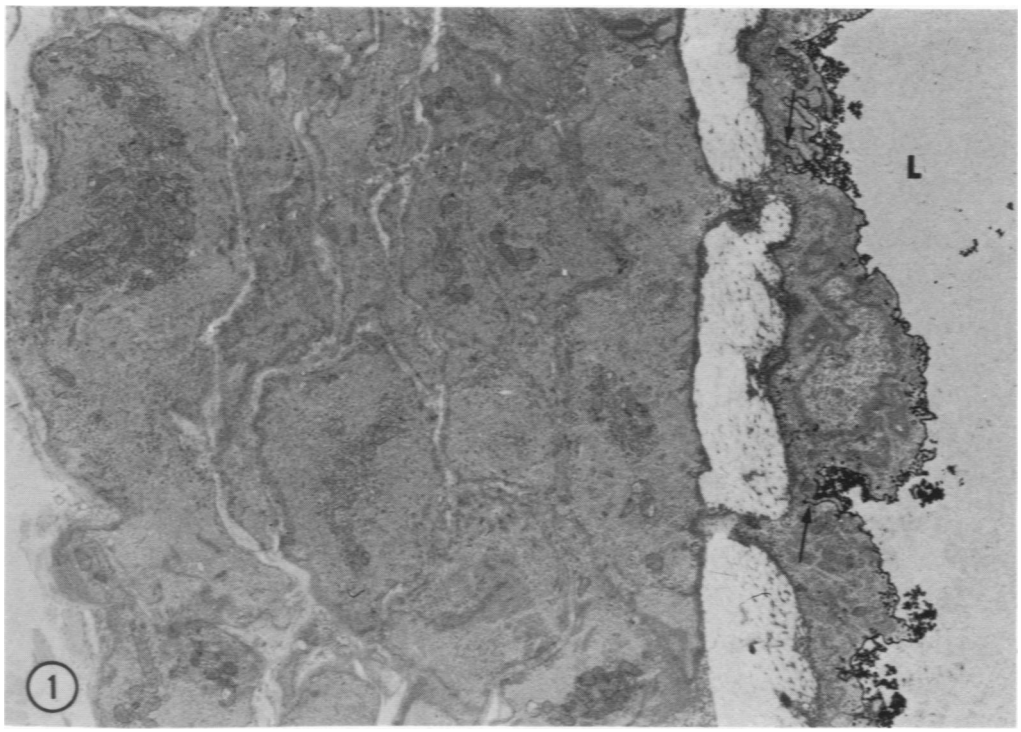
L
1

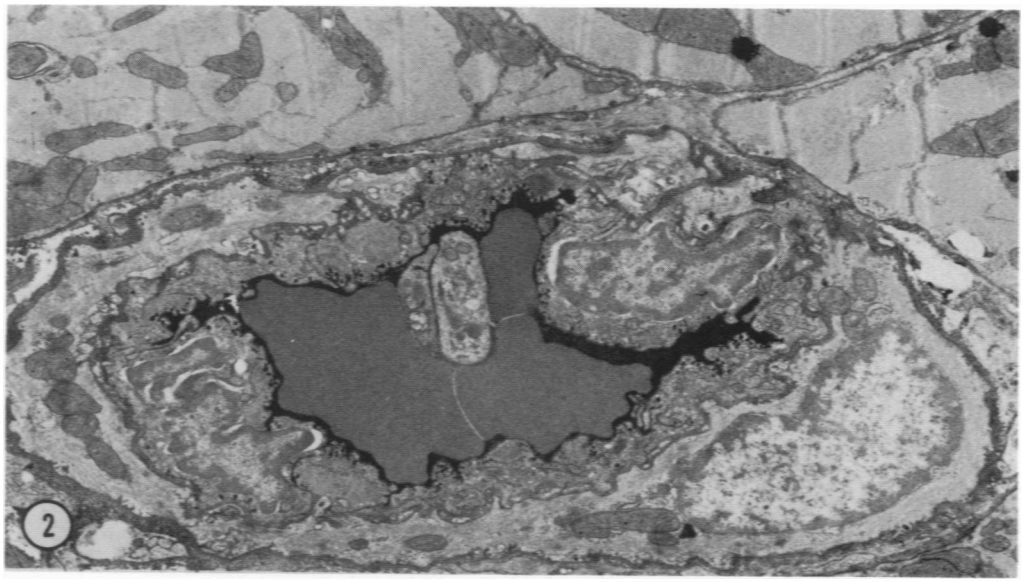
2

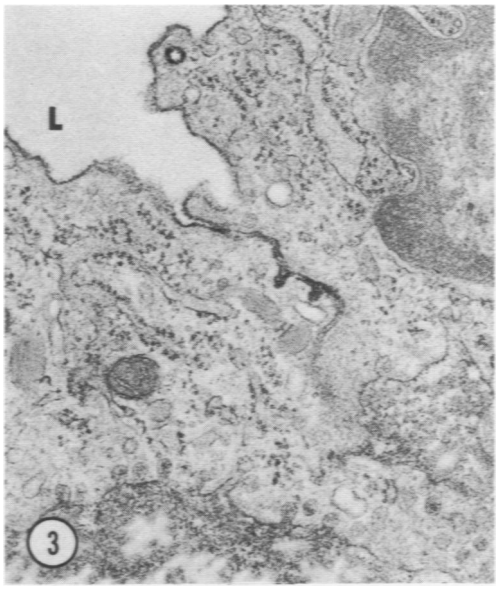
L
3

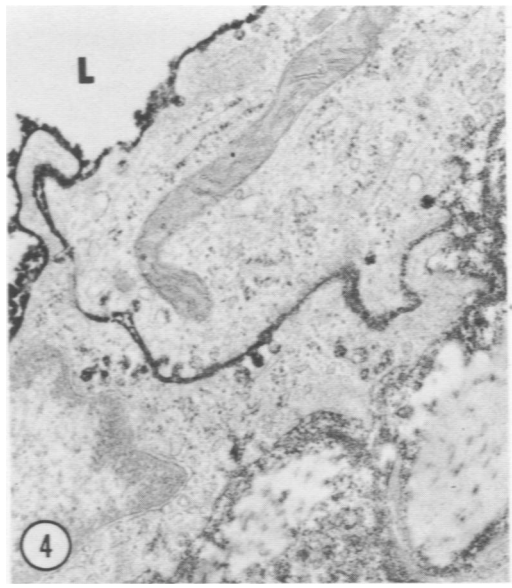
L
4

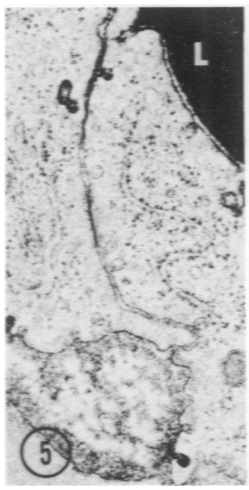
L
5


L
6

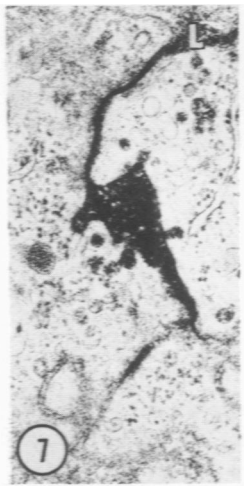
L
7

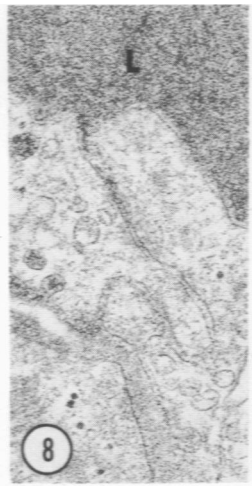
L
8

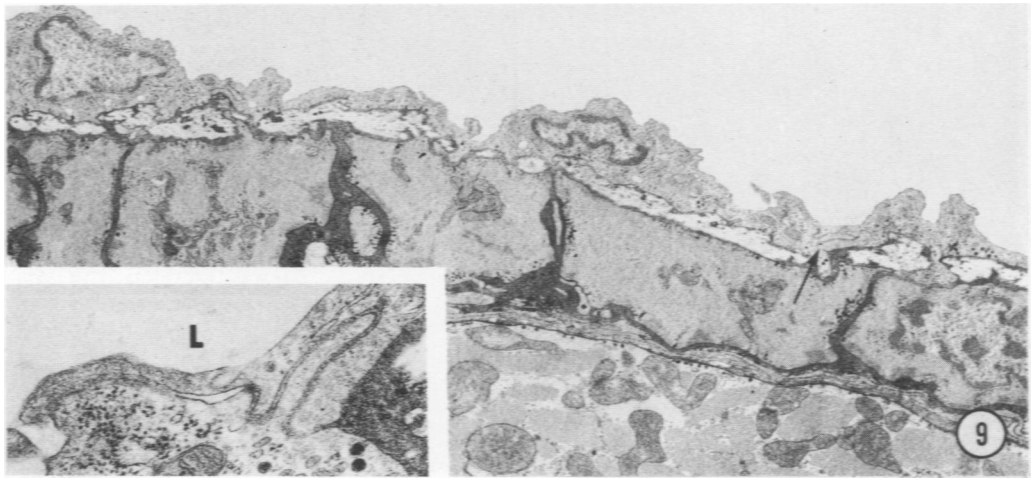
L
9

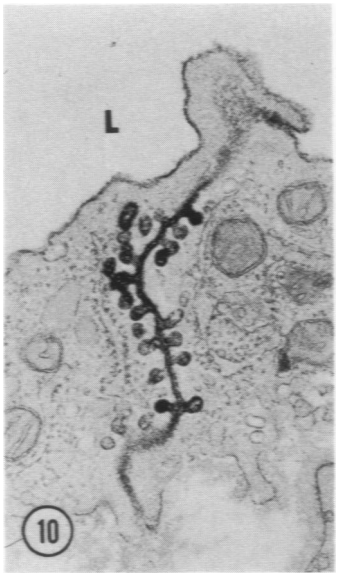
L
10

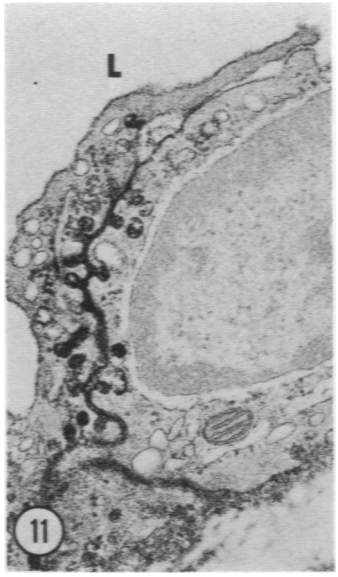
L
11

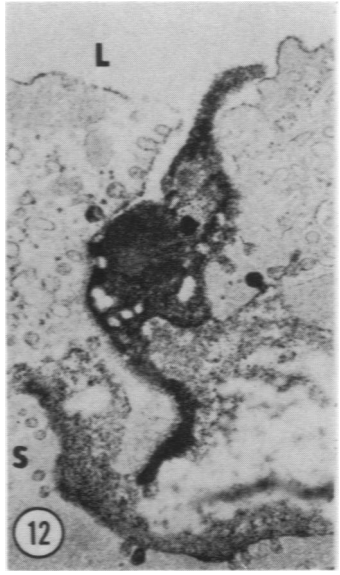
L
S
12

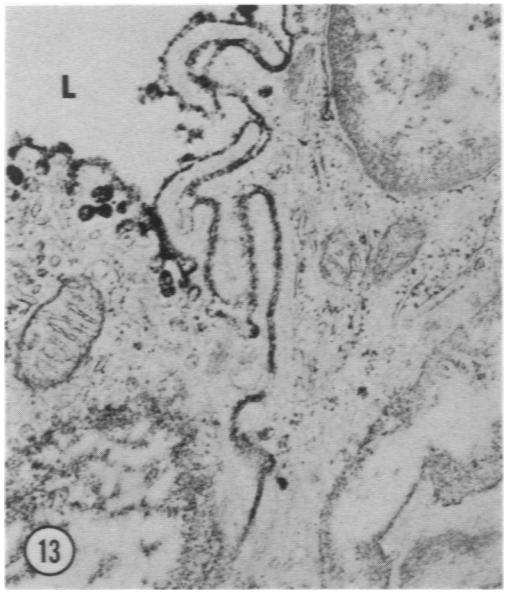
L
13

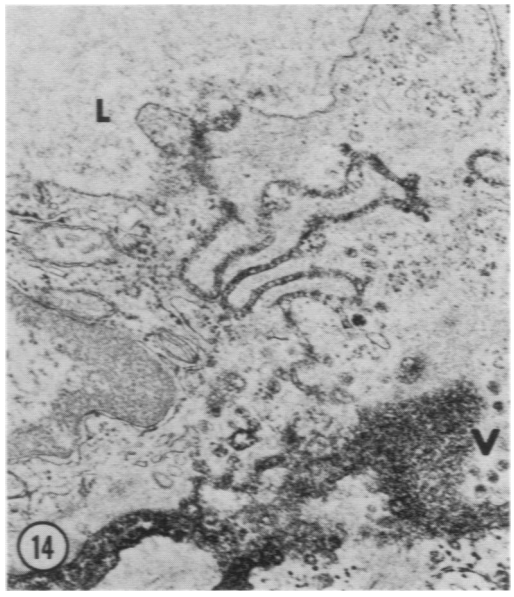
L
V
14

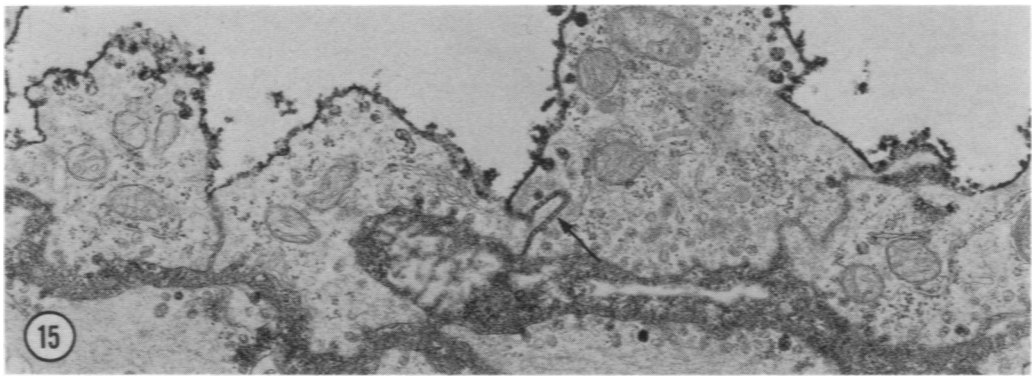
15

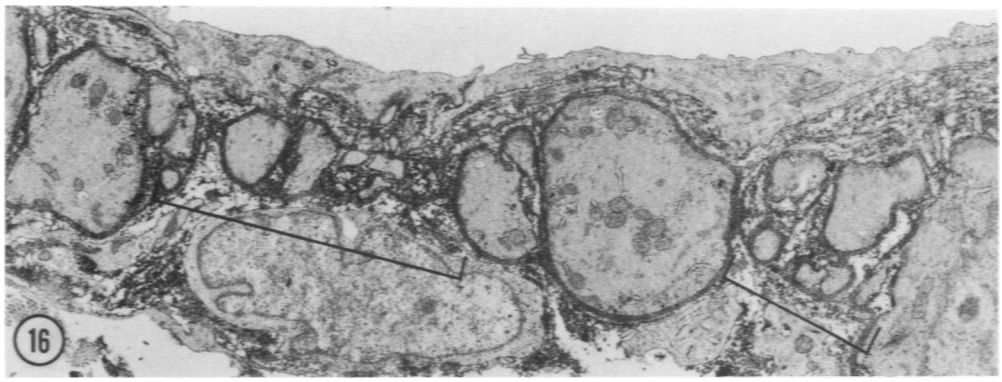

16

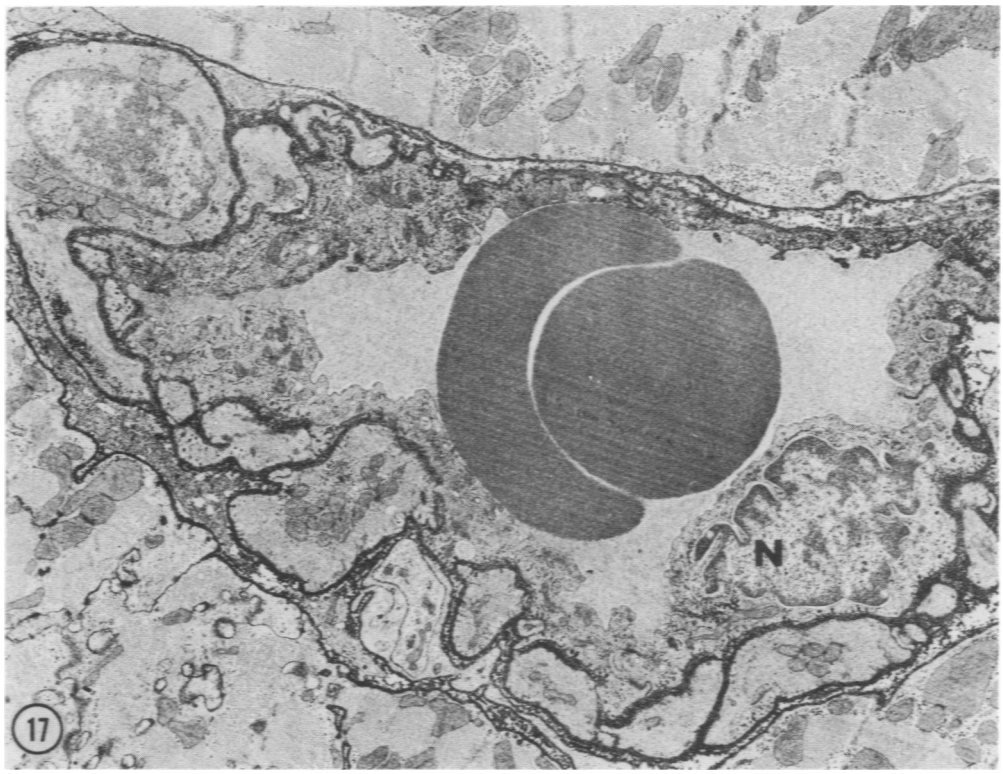

17

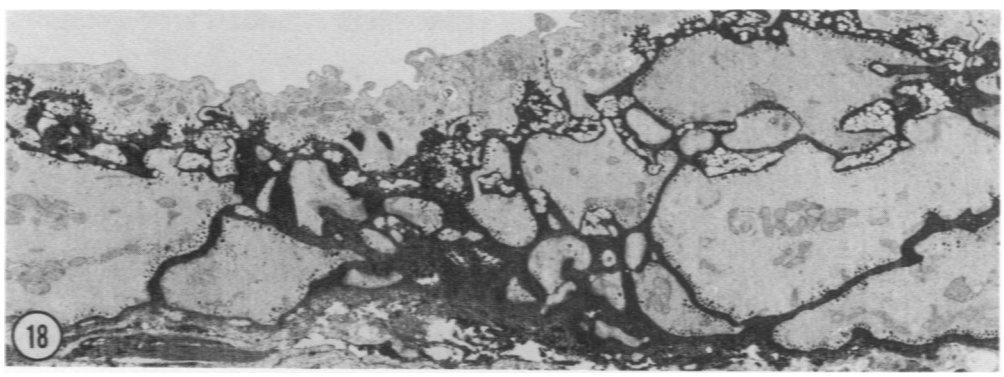

18

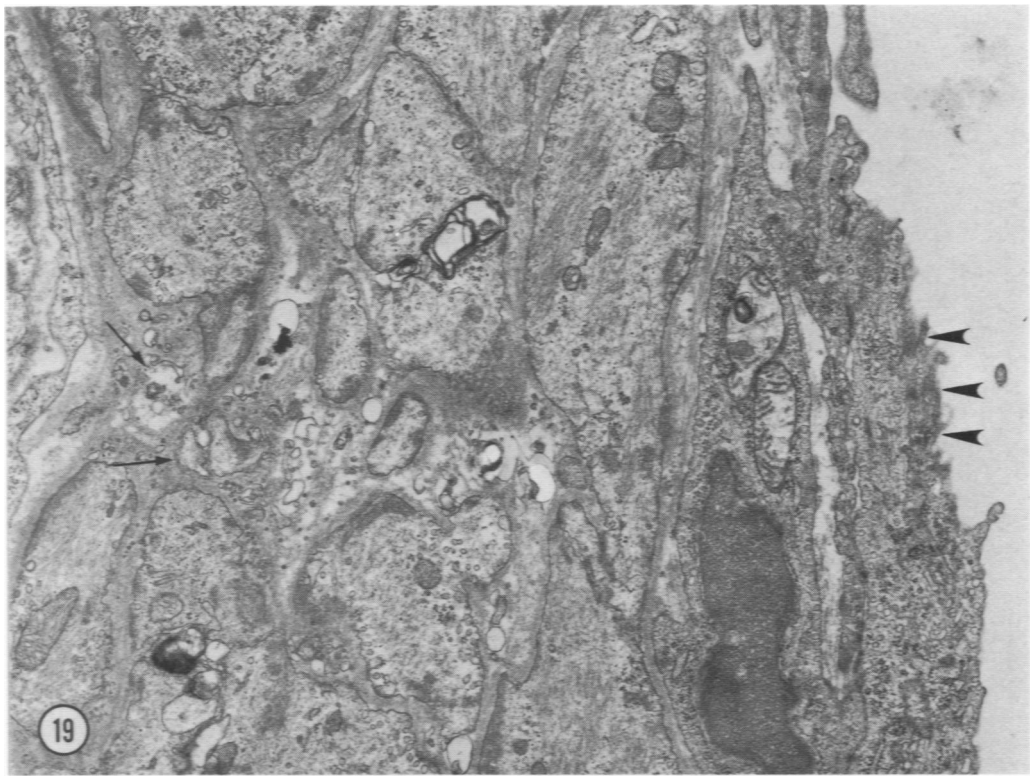
19

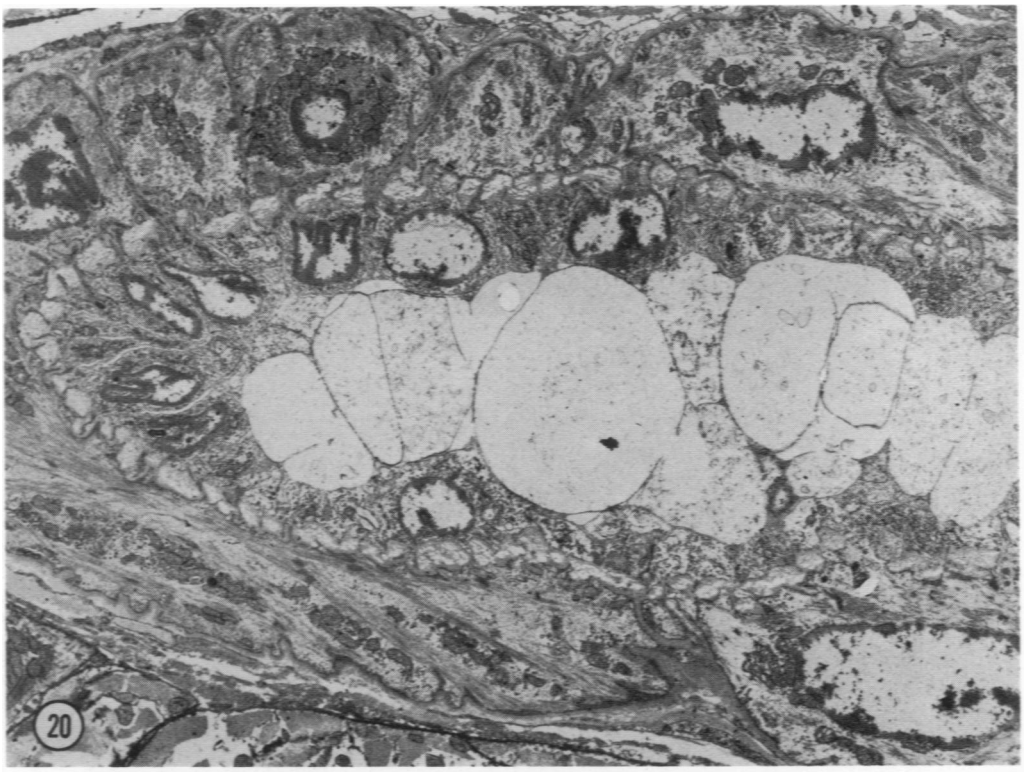
20

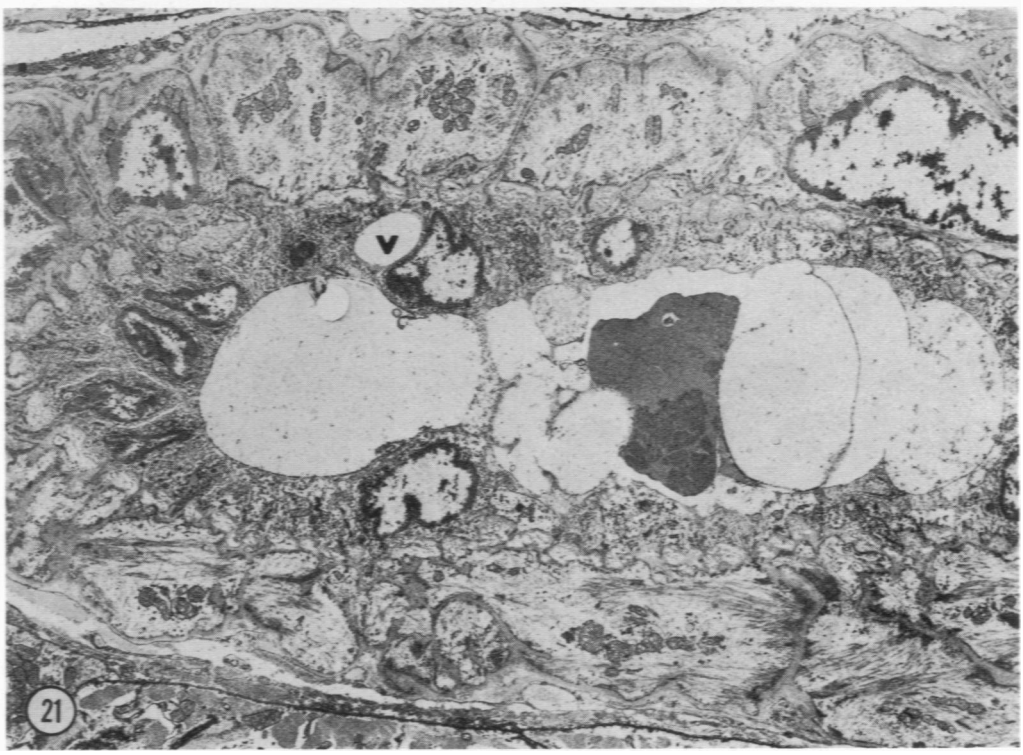
v
21

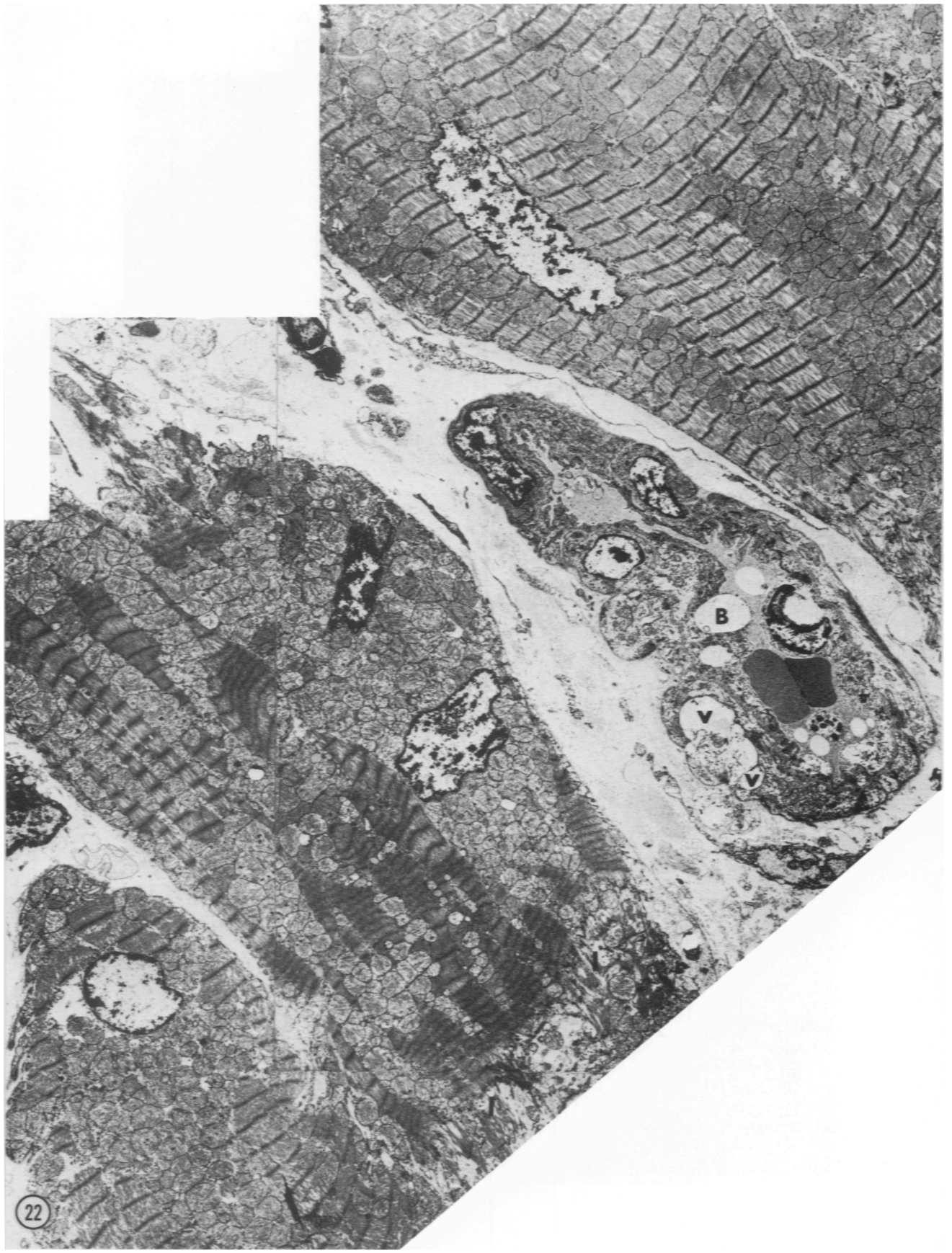

22

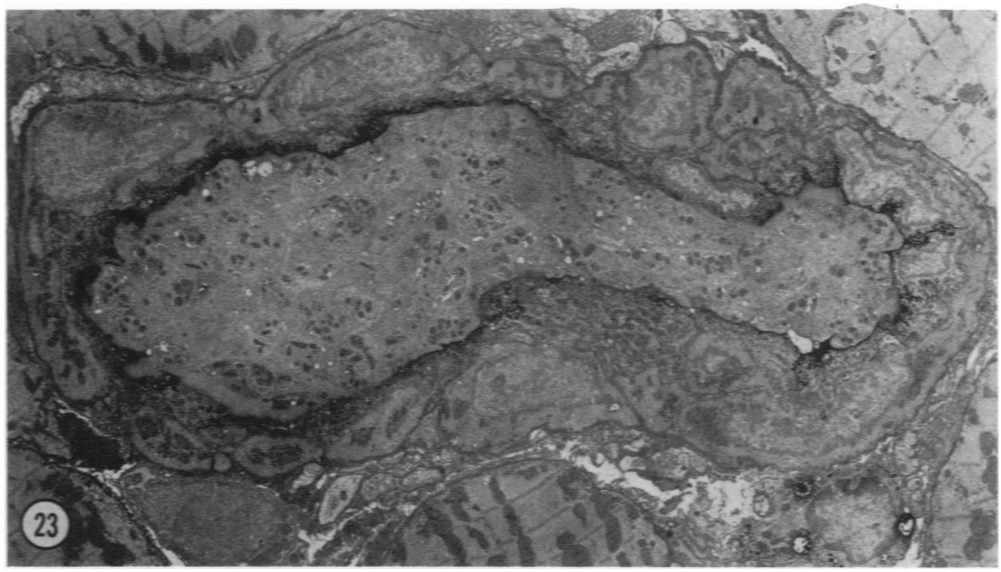
23

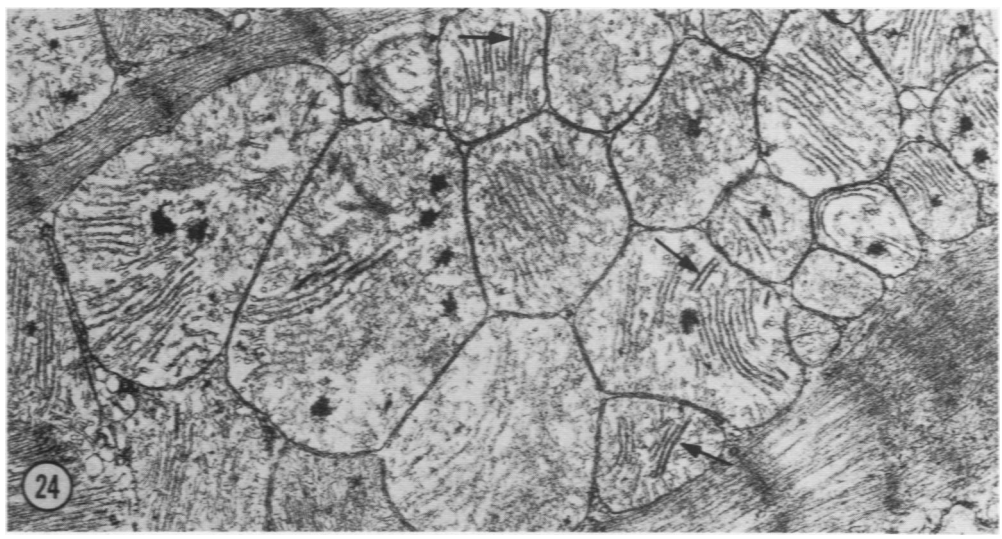
24

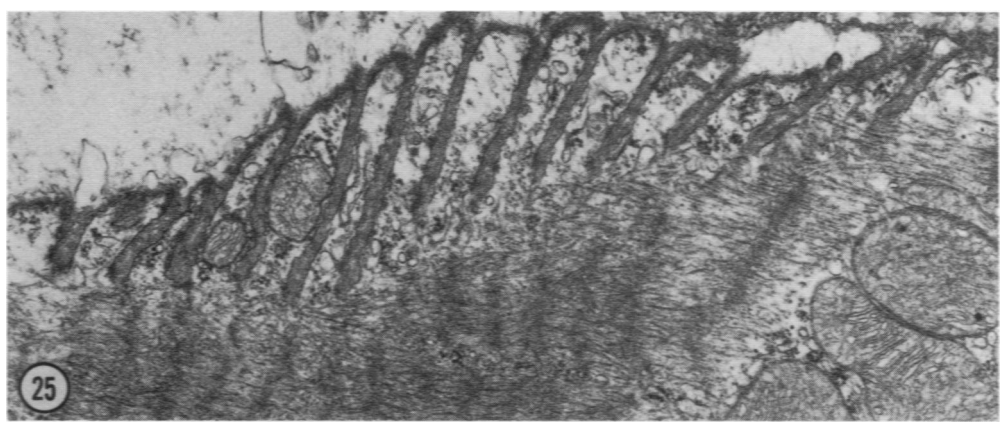
25

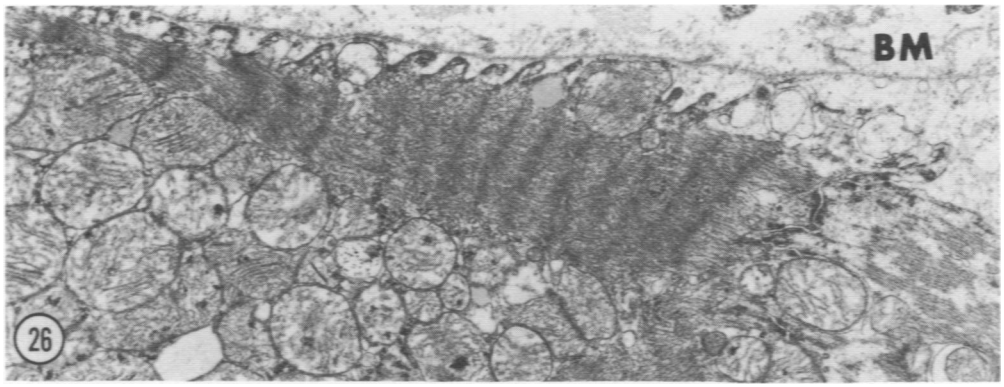

26

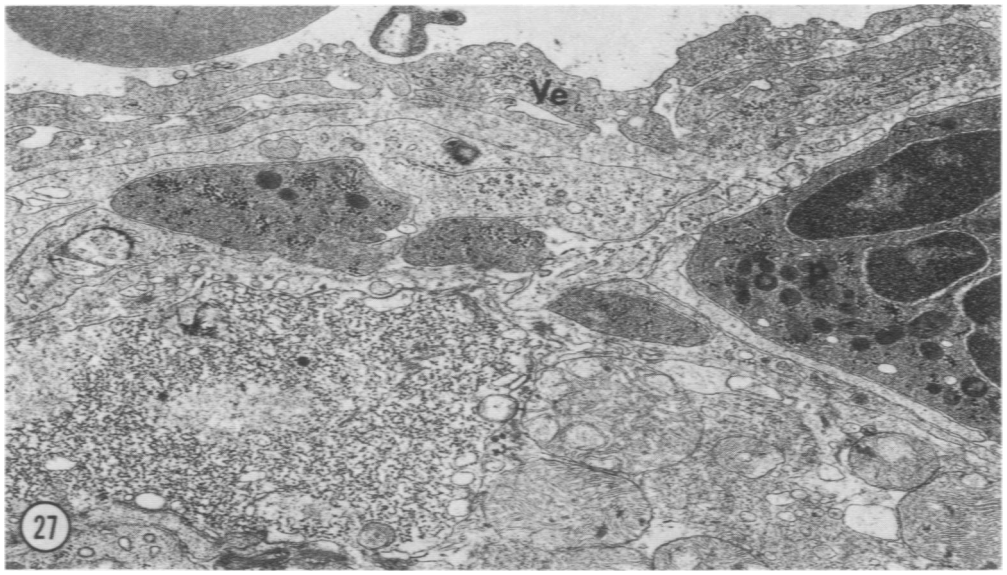

27

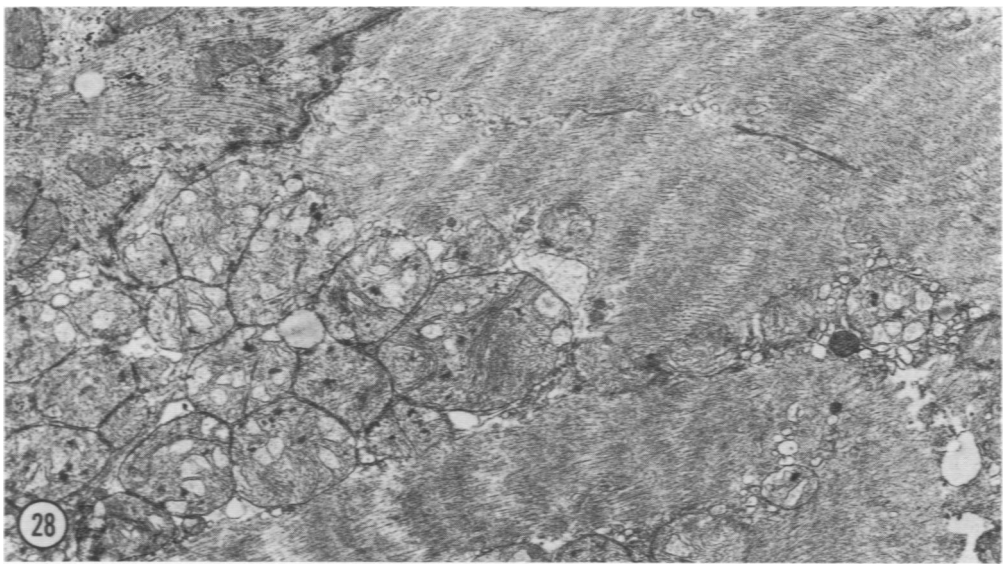

28

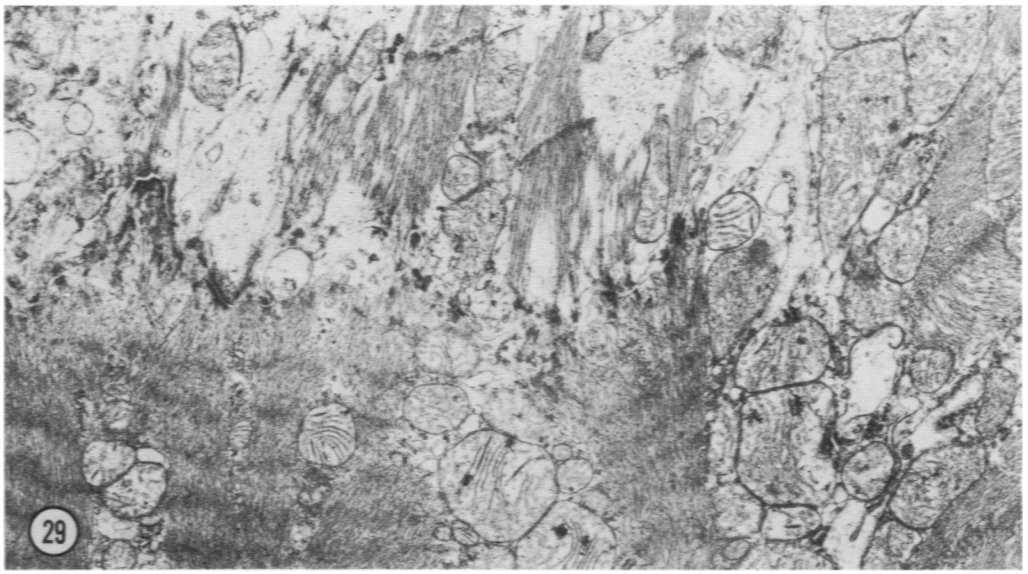
29

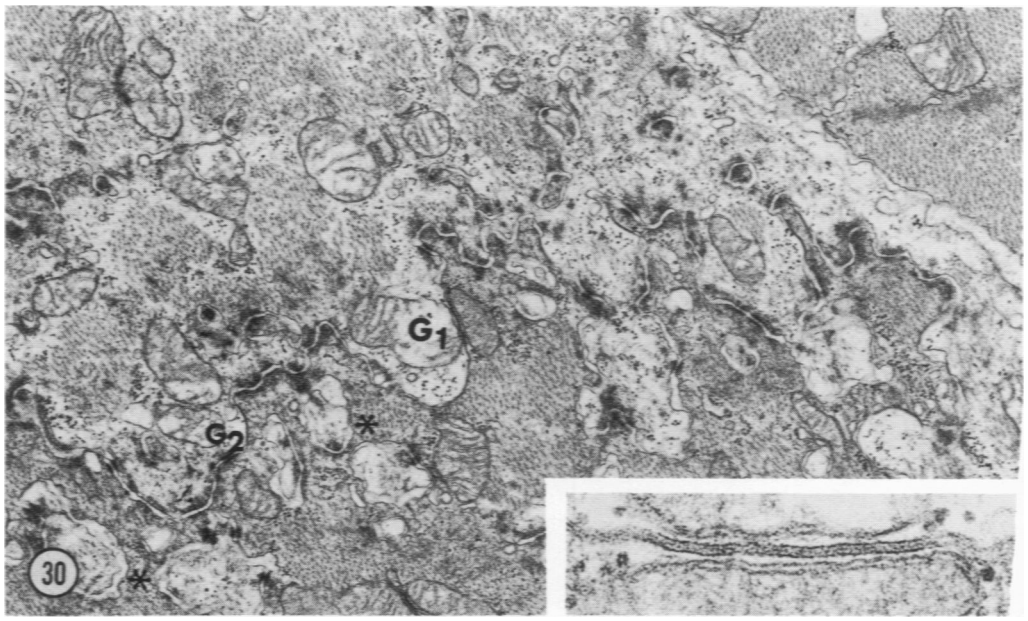
30
G1
G2
*
*